



NLRP11 disrupts MAVS signalosome to inhibit type I interferon signaling and virus-induced apoptosis

Yunfei Qin^{1,2,†}, Zexiong Su^{1,†}, Yaoxing Wu^{1,†} , Chenglei Wu¹, Shouheng Jin¹, Weihong Xie¹, Wei Jiang³, Rongbin Zhou³ & Jun Cui^{1,*} 

Abstract

MAVS signalosome plays an important role in RIG-I-like receptor (RLR)-induced antiviral signaling. Upon the recognition of viral RNAs, RLRs activate MAVS, which further recruits TRAF6 and other signaling proteins to initiate type I interferon (IFN) activation. MAVS signalosome also regulates virus-induced apoptosis to limit viral replication. However, the mechanisms that control the activity of MAVS signalosome are still poorly defined. Here, we report NLRP11, a Nod-like receptor, is induced by type I IFN and translocates to mitochondria to interact with MAVS upon viral infection. Using MAVS as a platform, NLRP11 degrades TRAF6 to attenuate the production of type I IFNs as well as virus-induced apoptosis. Our findings reveal the regulatory role of NLRP11 in antiviral immunity by disrupting MAVS signalosome.

Keywords apoptosis; MAVS; NLRP11; TRAF6; type I IFNs

Subject Categories Immunology; Microbiology, Virology & Host Pathogen Interaction; Signal Transduction

DOI 10.15252/embr.201744480 | Received 15 May 2017 | Revised 25 September 2017 | Accepted 4 October 2017 | Published online 2 November 2017

EMBO Reports (2017) 18: 2160–2171

Introduction

Innate immune responses against viral infection start with the recognition of pathogen-associated molecular patterns (PAMPs) by pattern-recognition receptors (PRRs), leading to the production of type I interferons (IFNs) [1]. The RIG-I-like receptor (RLR) family, including RIG-I, MDA5, and LGP2, are the primary PRRs to recognize viral RNAs and initiate antiviral responses [2]. Upon binding to viral RNA, RIG-I undergoes conformation change which subsequently leads to its interaction with MAVS [3]. MAVS then aggregates and serves as a platform for recruiting downstream proteins, including TRAF3, TRAF5, and TRAF6, to form a large signalosome [4,5]. Subsequently, the MAVS signalosome activates IRF3/7 and NF- κ B pathway, leading to the

production of type I IFNs (IFN α/β) and pro-inflammatory cytokines [5,6].

Sustained RLR activation results in extensive cell damage as well as the apoptosis via mitochondria-dependent mechanism [7,8]. It is generally accepted that apoptosis of infected cells is critical in suppression of viral replication and production of progeny viruses [9]. Recently, studies have clarified the essential roles of MAVS in the initiation of virus-induced apoptosis [7,10]. Thus, MAVS signalosome is also known as an important mediator in antiviral responses, due to its dual functions in virus-induced type I IFNs and apoptosis.

Nod-like receptors (NLRs) are a large family of cytosolic proteins activated by intracellular PAMPs and danger-associated molecular patterns (DAMPs) [11,12]. The best-characterized NLRs are NOD1 and NOD2, which initiate innate immune signaling by activating RIP2 via their CARD domains upon binding to PAMPs, leading to the activation of MAPK and NF- κ B signaling pathways [13]. Unlike NOD1 and NOD2, NLRP1, NLRP3, and NLRC4 form the large protein complexes called “inflammasome” with procaspase-1 to mediate the mature of IL-1 β and IL-18 [14]. In addition, recent studies have identified several NLRs functioned as negative regulators in innate immune responses, including NLRC5, NLRP4, NLRX1, and NLRC3, through diverse mechanisms [15–19]. However, the regulatory roles of several other NLRs in antiviral responses are still need to be characterized. In this study, we identified NLRP11 as a negative regulator in antiviral responses. Upon viral infection, NLRP11 is upregulated and translocates to mitochondria, and subsequently attenuating the activation of MAVS signalosome by promoting the degradation of TRAF6. Besides inhibiting IRF3 activation, NLRP11 also suppresses virus-induced apoptosis in a MAVS-dependent manner, which serves as a dual mediator to maintain homeostasis of innate antiviral responses.

Results

NLRP11 is a negative regulator of type I IFN signaling induced by RNA viruses

NLRP11 is a NLR protein which specifically exists in primates [20], and the biological function of NLRP11 in innate antiviral responses

1 Key Laboratory of Gene Engineering of the Ministry of Education, State Key Laboratory of Biocontrol, School of Life Sciences, Sun Yat-sen University, Guangzhou, China

2 School of Life Sciences, Zhengzhou University, Zhengzhou, Henan, China

3 Institute of Immunology and the CAS Key Laboratory of Innate Immunity and Chronic Disease, CAS Center for Excellence in Molecular Cell Sciences, School of Life Sciences and Medical Center, University of Science and Technology of China, Hefei, China

*Corresponding author. Tel: +86 20 39943429; E-mail: cuij5@mail.sysu.edu.cn

†These authors contributed equally to this work

remains unclear. We found poly(I:C)- and poly(dA:dT)-induced IFN-stimulated response element (ISRE) or IFN- β activation was remarkably attenuated by NLRP11 (Fig 1A and B). Similarly, overexpression of NLRP11 inhibited Sendai virus (SeV, a RNA virus)-induced ISRE or IFN- β activation (Fig 1C). Since both RNA and DNA viral infection activated the productions of type I IFNs, we also examined the functions of NLRP11 in IFN pathway induced by cGAS, which has been identified as a cytosolic sensor for DNA viruses through the adaptor STING [21]. However, NLRP11 barely affected cGAS-induced IFN- β promoter activation via STING-dependent pathway (Fig 1D). These results suggested NLRP11 specifically suppressed RLR-mediated type I IFN signaling. To confirm the antiviral function of NLRP11, we constructed *NLRP11* overexpressing and knockdown (shNLRP11) THP-1 cell lines, respectively (Fig EV1A and B). Knockdown of *NLRP11* enhanced IRF3 phosphorylation upon SeV, but not Herpes simplex virus type 1 (HSV-1, a DNA virus) infection (Figs 1E and EV1C). In addition, the mRNA levels of *IFNB1*, *IFN-stimulated gene 54* (*ISG54*), and *IFN-stimulated gene 56* (*ISG56*) were inversely associated with the amount of NLRP11 after SeV infection (Figs 1F and G, and EV1D). In order to investigate the function of NLRP11 in primary cells, we knocked down endogenous *NLRP11* in human peripheral blood mononuclear cells (PBMCs) by *NLRP11*-specific siRNAs, and found that the expressions of *IFNB1* and its downstream molecules *ISG54* and *ISG56* were enhanced, but *SeV phosphoprotein* expression was decreased in *NLRP11*-knockdown PBMCs (Fig EV1E). Moreover, IFN- β protein secretion was also increased in *NLRP11*-knockdown PBMCs upon SeV infection (Fig EV1F). Collectively, our finding suggested that knockdown of *NLRP11* enhanced type I IFN signaling induced by RLRs.

NLRP11 deficiency enhances IFN- β expression as well as antiviral responses

To further confirm the negative role of NLRP11 in RLR-induced antiviral responses, we constructed *NLRP11* knockout (KO) 293T and THP-1 cells, respectively, by the clustered regulatory interspersed short palindromic repeat (CRISPR)/CRISPR-associated protein (Cas) system [22]. The KO efficiency of *NLRP11* was confirmed by immunoblot analysis and DNA sequencing (Fig EV2A and B). ISRE or IFN- β activation was enhanced in *NLRP11* KO cells after poly(I:C), poly(dA:dT) treatment, or SeV infection (Fig 2A and B). Next, we expressed a sgRNA-resistant version of *NLRP11* in *NLRP11* KO cells and found it can reverse the enhancement of type I IFN activation caused by NLRP11 deficiency (Fig EV2C). In *NLRP11* KO THP-1 cells, the phosphorylation of IRF3 was enhanced compared to wild-type (WT) cells upon SeV infection (Fig 2C). Consistently, the mRNA levels of *IFNB1*, *ISG54*, and *ISG56* in *NLRP11* KO THP-1 cells were significantly increased after SeV, but not HSV-1 infection (Figs 2D and EV2D). Moreover, pro-inflammatory cytokines, such as *IL6* and *TNFA*, were also upregulated in *NLRP11* KO THP-1 cells upon SeV infection (Fig EV2E). As expected, we found that NLRP11 deficiency reduced the number of GFP-positive cells compared with WT THP-1 cells upon vesicular stomatitis virus tagged with enhanced green fluorescent protein (VSV-eGFP) infection (Fig 2E and F). Taking together, these data suggested that NLRP11 was a specific negative regulator in RLR pathway and limited the production of antiviral cytokines during antiviral immunity.

NLRP11 inhibits IRF3 activation by targeting MAVS

To determine the molecular mechanisms by which NLRP11 inhibits type I IFN signaling, we co-transfected 293T cells with expression vectors encoding RIG-I (CARD) (an active domain of RIG-I), MDA5, MAVS, TBK1, or IRF3 (5D) (a constitutively active mutant of IRF3) together with the ISRE luciferase reporter and the increasing amounts of NLRP11. We found that NLRP11 inhibited ISRE reporter activity induced by RIG-I (CARD), MDA5 and MAVS, but not TBK1 or IRF3 (5D) (Figs 3A and EV3A). We also found NLRP11 inhibited IRF3 dimerization induced by RIG-I (CARD) and MAVS, but not TBK1 (Fig EV3B). These results suggested that NLRP11 markedly inhibited type I IFN signaling at MAVS level. Next, we sought to determine whether NLRP11 could directly interact with MAVS or other signaling proteins within the type I IFN pathway. Co-immunoprecipitation (Co-IP) experiments revealed that NLRP11 strongly interacted with MAVS (Fig 3B). Moreover, endogenous NLRP11 weakly interacted with MAVS in THP-1 cells, while the interaction between NLRP11 and MAVS was notably increased upon SeV infection (Fig 3C). Since NLRP11 expression was upregulated after SeV infection (Fig 3C), we overexpressed NLRP11 in 293T cells to eliminate the expression differences of NLRP11 during viral infection and found that the interaction between NLRP11 and MAVS was consistently enhanced during SeV infection (Fig EV3C). These results indicated that NLRP11 associated with MAVS during viral infection. Next, we investigated which domain of MAVS was responsible for its interaction with NLRP11. Since the CARD domain of MAVS is essential for RIG-I-MAVS interaction and transmembrane (TM) domain is critical for MAVS's mitochondria localization [23], we generated two MAVS deletion mutants, MAVS- Δ CARD and MAVS- Δ TM, respectively (Fig 3D). We found that the CARD deletion mutant markedly reduced the interaction between NLRP11 and MAVS (Fig 3E). In addition, the TM domain of MAVS was also essential for its interaction with NLRP11, since the deletion of TM domain in MAVS (MAVS- Δ TM) completely abolished NLRP11-MAVS interaction (Fig 3E). These results indicated that both TM domain and CARD domain of MAVS were important for its interaction with NLRP11. TM domain guaranteed the mitochondria localization of MAVS to allow NLRP11 to approach it upon viral infection, while MAVS might directly interact with NLRP11 through its CARD domain. To identify the functional domains of NLRP11, we generated three domain constructs of NLRP11: NLRP11-PYD, NLRP11-NOD, and NLRP11-LRR (Fig 3F). NOD and LRR, but not PYD, could interact with the full-length MAVS protein (Fig 3G), as well as inhibit the ISRE activity induced by MAVS (Fig 3H). These results suggested that NLRP11-LRR and NLRP11-NOD were required for its binding ability with MAVS.

NLRP11 targets TRAF6 for degradation in MAVS signalosome

Next, we investigated how NLRP11 negatively regulated MAVS-mediated antiviral responses. Co-IP assays showed NLRP11 did not disrupt the interaction between MAVS and its upstream molecule, RIG-I (Fig EV3D). In addition, overexpression of NLRP11 barely affected the ubiquitination of MAVS (Fig EV3E), which is an important signal for MAVS activation in type I IFN signaling [5]. It has been reported that MAVS polymers recruited multiple TRAF proteins to form MAVS signalosome, which finally led to activation

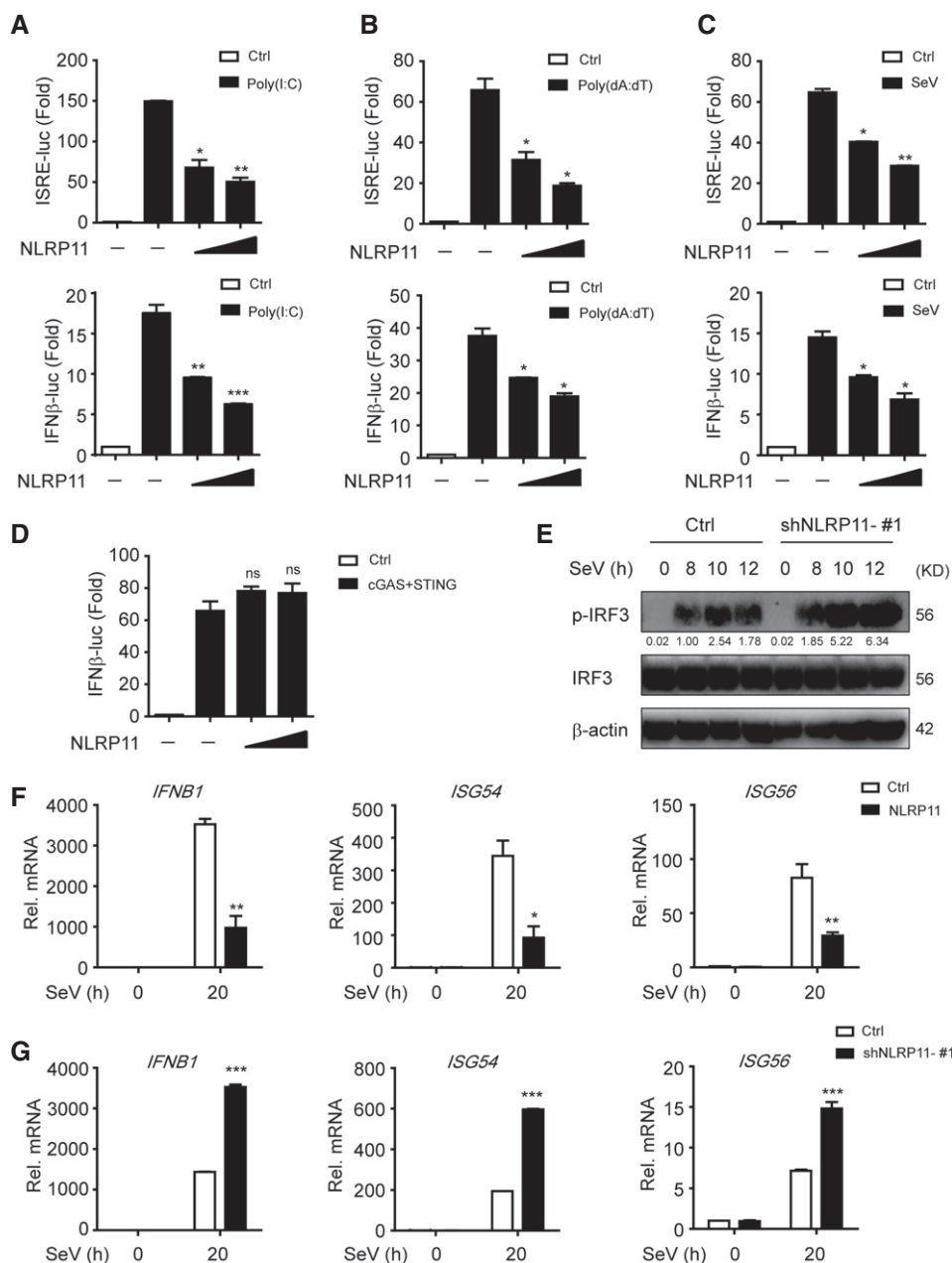


Figure 1. NLRP11 inhibits the activation of type I IFN signaling.

A–C 293T cells were transfected with an ISRE or IFN- β promoter reporter plasmid and pRL-TK plasmid, together with an empty vector (EV) or NLRP11 construct for 24 h, and then transfected with poly(I:C) (5 μ g/ml) (A), poly(dA:dT) (5 μ g/ml) (B), or infected with Sendai virus (SeV) (MOI = 0.1) for 20 h (C), followed by ISRE- or IFN- β -dependent luciferase activity (fold induction) analysis. The data were normalized by using the values of ISRE-luc or IFN- β -luc divided by the values of TK-luc, and then, the results of each group were analyzed to compare with the control group.

D 293T cells were transfected with the IFN- β promoter reporter plasmid and pRL-TK plasmid, together with an empty vector or cGAS and STING plasmids and increasing amount of NLRP11 for 24 h, and analyzed for IFN- β -dependent luciferase activity (fold induction).

E Immunoblot analysis of the total and phosphorylated (p-) IRF3 in THP-1 cells stably transduced with recombinant lentivirus expressing empty vector or shNLRP11-#1, which were left untreated or infected with SeV (MOI = 1) for indicated time points. Numbers between two blots indicate densitometry of phosphorylated proteins relative to that of total proteins, respectively.

F, G Expression of *IFNB1*, *ISG54*, and *ISG56* mRNA in NLRP11 overexpressing THP-1 cells (F) or NLRP11-knockdown THP-1 cells (G) infected with SeV (MOI = 1) for indicated time points.

Data information: Data in (A–D, F, and G) are expressed as means \pm SEM of three independent experiments (* P < 0.05, ** P < 0.01, and *** P < 0.001, versus cells transfected with EV with the same treatment, Student's t -test, ns: no significant).

Source data are available online for this figure.

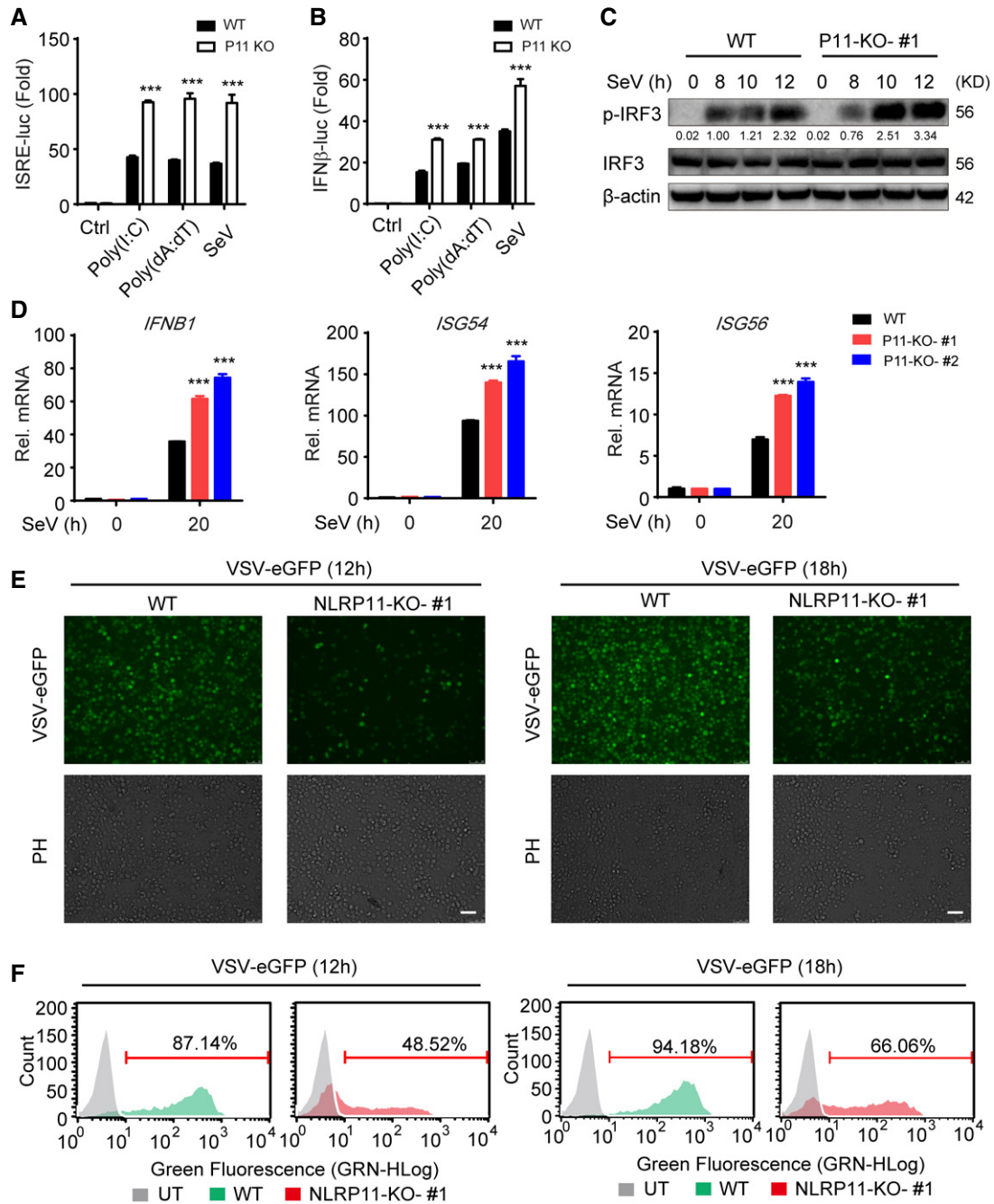


Figure 2. Knockout of *NLRP11* enhances the production of IFN-β and antiviral responses.

A, B Wild-type (WT) and *NLRP11* knockout (KO) 293T cells were transfected with an ISRE (A) or IFN-β (B) promoter reporter plasmid and pRL-TK plasmid for 24 h, and then transfected with poly(I:C) (5 μg/ml) (A), poly(dA:dT) (5 μg/ml), or infected with Sendai virus (SeV) (MOI = 0.1) for 20 h, followed by ISRE- or IFN-β-dependent luciferase activity (fold induction) analysis.

C WT and *NLRP11* KO THP-1 cells were infected with SeV (MOI = 1) for indicated time points, and total and phosphorylated (p-) IRF3 were analyzed by immunoblot analysis. Numbers between two blots indicate densitometry of phosphorylated proteins relative to that of total proteins, respectively.

D WT and *NLRP11* KO THP-1 cells were infected with SeV (MOI = 1) for 20 h, and then, *IFNB1*, *ISG54*, and *ISG56* induction were measured by real-time PCR.

E, F WT and *NLRP11* KO THP-1 cells were infected with VSV-eGFP (MOI = 10) for 12 h or 18 h, followed by phase-contrast (PH) and fluorescence microscopy analysis (E) and flow cytometric analysis (F). Numbers above bracketed lines indicated the percentage of VSV-eGFP-infected cells. Scale bar, 100 μm.

Data information: Data in (A, B, and D) are expressed as means ± SEM of three independent experiments (***) $P < 0.001$ versus WT cells with the same treatment, Student's *t*-test.

Source data are available online for this figure.

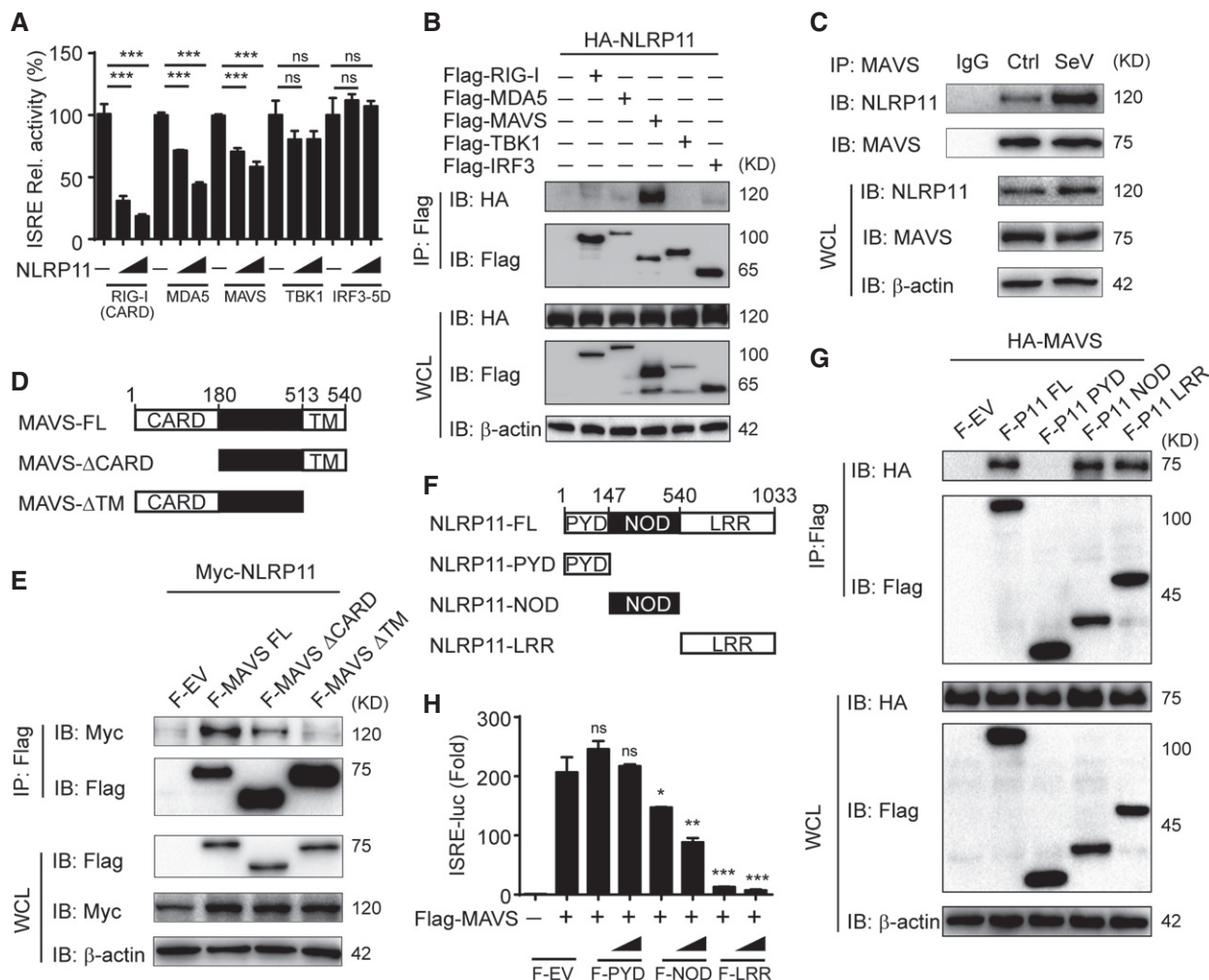


Figure 3. NLRP11 associates with MAVS to inhibit IRF3 activation.

A Luciferase activity in 293T cells transfected with the ISRE promoter reporter plasmid and pRL-TK plasmid for 24 h, together with expression plasmids encoding RIG-I-CARD, MDA5, MAVS, TBK1, and IRF3 (5D), and increasing amount of NLRP11.

B 293T cells were transfected with HA-NLRP11 and Flag-RIG-I, Flag-MDA5, Flag-MAVS, Flag-TBK1, and Flag-IRF3 for 24 h, and cell lysates were subjected to immunoprecipitation with anti-Flag beads, followed by immunoblot analysis with indicated antibodies.

C NLRP11 and MAVS interaction was analyzed by co-immunoprecipitation assay in THP-1 monocytes upon Sendai virus (SeV) (MOI = 1) infection for 20 h.

D The domain structure of MAVS. Numbers in parentheses indicate amino acid position in the construct.

E 293T cells were transfected with Myc-NLRP11 and Flag-MAVS, Flag-MAVS-ΔCARD, and Flag-MAVS-ΔTM for 24 h, and cell lysates were subjected to immunoprecipitation with anti-Flag beads, followed by immunoblot analysis with indicated antibodies.

F The domain structure of NLRP11. Numbers in parentheses indicate amino acid position in the construct.

G 293T cells were transfected with HA-MAVS and Flag-NLRP11, Flag-NLRP11-PYD, Flag-NLRP11-NOD, and Flag-NLRP11-LRR for 24 h, and cell lysates were subjected to immunoprecipitation with anti-Flag beads, followed by immunoblot analysis with indicated antibodies.

H Luciferase activity in 293T cells transfected with the ISRE promoter reporter, pRL-TK plasmid, and MAVS or empty vector (EV), together with expression plasmids encoding Flag-NLRP11-PYD, Flag-NLRP11-NOD, or Flag-NLRP11-LRR for 24 h.

Data information: Data in (A and H) are expressed as means \pm SEM of three independent experiments (* P < 0.05, ** P < 0.01, and *** P < 0.001, versus the cells transfected with EV with the same treatment, Student's t -test).

Source data are available online for this figure.

of NF- κ B and IRF3 [5,6,23]. Then, we examined the interaction of NLRP11 and TRAFs. Co-IP assays showed NLRP11 strongly interacted with TRAF6, rather than TRAF3 or TRAF5 (Fig 4A). We found TRAF6 is necessary for activating type I IFNs, and NLRP11 solely inhibited TRAF6-induced ISRE activation in human cells (Fig EV4A and B). The interaction between NLRP11 and TRAF6 was further determined by endogenous co-IP assay (Fig 4B). Our data revealed

that the association between NLRP11 and TRAF6 was also markedly increased upon SeV infection (Fig EV4C). In TRAF6 KO 293T cells, NLRP11 failed to inhibit the ISRE promoter activity induced by SeV infection (Fig 4C). These findings suggested that TRAF6 was critical for NLRP11-mediated inhibition of IFN activation.

When TRAF6 and NLRP11 or NLRP4 were overexpressed in 293T cells, we observed that TRAF6 expression was lower in the presence

of increasing amounts of NLRP11, but not NLRP4 (Fig EV4D). This finding prompted us to investigate the effect of NLRP11 on TRAF6 abundance. Next, we observed that endogenous TRAF6 protein level was decreased in *NLRP11* overexpressing THP-1 or 293T cells upon SeV infection (Figs 4D and EV4E). Consistently, TRAF6 was stabilized in *NLRP11* KO cells by SeV infection in the presence of cycloheximide (CHX) (Fig EV4F). We also found that the proteasome inhibitor MG132, but not the autophagic sequestration inhibitor 3-methyladenine (3-MA) or the lysosomal acidification inhibitor bafilomycin A1 (Baf A1), inhibited the degradation of TRAF6 mediated by NLRP11 (Fig EV4G). Moreover, NLRP11 enhanced the K48-, but not K63-linked ubiquitination of endogenous TRAF6 upon SeV infection (Figs 4E and EV4H). These results suggested that NLRP11 induced the degradation of TRAF6 through enhancing its K48-linked ubiquitination.

Since NLRP11 targets MAVS to inhibit IFN signaling (Fig 3B–E), we speculated whether MAVS plays as a platform for NLRP11 to degrade TRAF6. Indeed, MAVS deficiency abolished NLRP11-induced TRAF6 degradation (Fig 4F). In addition, co-IP assay showed that the interaction between NLRP11 and TRAF6 was remarkably suppressed in *MAVS* KO cells (Fig 4G). Taken together, these results indicated that NLRP11 regulated TRAF6 degradation in a MAVS-dependent manner.

Virus infection induces NLRP11 expression and its mitochondria translocation

Immunoblot analysis showed that NLRP11 protein level is upregulated upon SeV infection (Figs 3C and 4B). To confirm it, we treated the THP-1 and HeLa cells with poly(I:C) or SeV infection. We found that SeV infection and poly(I:C) stimulation increased NLRP11 mRNA and protein level in THP-1 and HeLa cells (Figs 5A and B, and EV5A and B). As both poly(I:C) and SeV activate type I IFN signaling, we speculated that NLRP11 expression might rely on type I IFN secretion. Indeed, IFN- β treatment increased NLRP11 expression in THP-1 and HeLa cells (Figs 5C and EV5C), indicating that NLRP11 is an ISG gene, which can form a negative feedback loop to regulate type I IFN signaling.

Next, we transfected GFP-NLRP11 into 293T cells to investigate the cellular localization of NLRP11. NLRP11 showed diffused expression in cytoplasm in resting cells (Figs 5D and EV5D). However, a proportion of NLRP11 aggregated after SeV infection or poly(I:C) treatment (Figs 5D and EV5D). It has been reported that RLR activation induced the prionlike polymerization of MAVS on mitochondria, which recruited downstream adaptors to amplify signaling [4,23]. We also found TM domain deletion of MAVS did not interact with NLRP11 anymore (Fig 3E). Based on these results, we reasoned that NLRP11 may aggregate on mitochondria. To test this hypothesis, we performed mitochondria isolation analysis and found that a fraction of NLRP11 translocated from cytosol to mitochondria upon SeV infection (Fig 5E).

NLRP11 suppresses virus-induced apoptosis

Apoptosis is an important part of host defending to limit virus replication and spreading [24]. It has been reported that MAVS and TRAF6 have central roles in mediating the apoptosis of virus-infected cells [25]. Since we found NLRP11 disrupted MAVS signalosome by promoting TRAF6 degradation, we reasoned that NLRP11

may also regulate virus-mediated apoptosis. To test this hypothesis, we infected WT or *NLRP11* KO THP-1 cells with VSV-eGFP at a multiplicity of infection (MOI) of 10. We observed that trypan blue-positive cells (dead cells) significantly increased in *NLRP11* KO group (Fig 6A), indicating the potential inhibitory functions of NLRP11 on apoptotic cell death. Similarly, *NLRP11* KO THP-1 cells have a higher propidium iodide (PI) staining after VSV-eGFP infection, as compared to WT cells (Fig 6B). In addition, a greater percentage of PI staining-positive cells was observed in the absence of NLRP11 by flow cytometry analysis (Fig 6C). We next examined the effect of NLRP11 on poly-ADP-ribose polymerase (PARP) cleavage and observed that overexpression of NLRP11 reduced the cleavage of PARP upon VSV-eGFP infection (Fig 6D). In addition, we found that the effect of NLRP11 on PARP cleavage is dependent on MAVS (Fig 6E). Consistently, an increasing cleavage of PARP was observed in *NLRP11* KO cells after VSV-eGFP infection, as compared to WT cells (Fig 6F). It has been reported that VSV M protein is a potent inhibitor of host gene expression, which could also trigger apoptosis of infected cells [26]. In order to remove the apoptosis mediated by M protein, we transfected poly(I:C) to induce apoptosis. We observed more apoptotic cells by viral infection when *NLRP11* was knocked down (Fig 6G and H). However, knockdown of *TRAF6* abrogated the inhibition of poly(I:C)-induced apoptosis mediated by NLRP11 (Fig 6I). Taken together, our finding indicated that NLRP11 attenuated virus or poly(I:C)-induced apoptosis in a MAVS- and TRAF6-dependent manner.

Discussion

NOD-like proteins are involved in the activation of diverse innate immune signaling pathways [11,12]. NOD1, NOD2, NLRP1, NLRP3, and NLRC4 have been extensively studied and shown to activate MAPK and NF- κ B pathways or form inflammasomes once they encounter relevant PAMPs [13,14]. Recently, accumulating evidence revealed the negative regulatory roles of NLRs in immune responses. NLRP12 has been reported to be involved in the regulation of inflammation [27,28]. We and others found that NLRX1 inhibits RNA virus-induced type I IFN signaling and NF- κ B pathway by binding to MAVS and IKK complex, respectively [17,29]. We also found NLRC5 plays a critical role in the negative regulation of intracellular antiviral responses via interaction with RLRs [15], whereas NLRP4 reduces IFN production through promoting TBK1 degradation [16,18]. However, the role of NLRP11 in the regulation of antiviral immunity remains unknown. In this study, we report that NLRP11 serves as a negative regulator of type I IFN pathway and apoptosis by targeting MAVS signalosome for degradation of TRAF6 upon viral infection.

MAVS is a mitochondria adaptor protein, which acts as a major adaptor for RLRs [2]. Upon viral infection, RLRs initiate the aggregation of MAVS [4]. MAVS then recruits distinct TRAFs to form MAVS signalosome, which in turn activates IRF3/7 and NF- κ B pathway or apoptosis [5–7,25]. Up to now, the function of TRAF6 in type I IFN signaling is still under debate. Chattopadhyay *et al* [25] found TRAF6 was not necessary for IRF-3-mediated gene induction induced by poly(I:C) in MEFs. However, several other groups and our studies have clarified the essential roles of TRAF6 in virus-induced IFN signaling (Fig EV4A) [23,30]. Chen *et al* [30] found

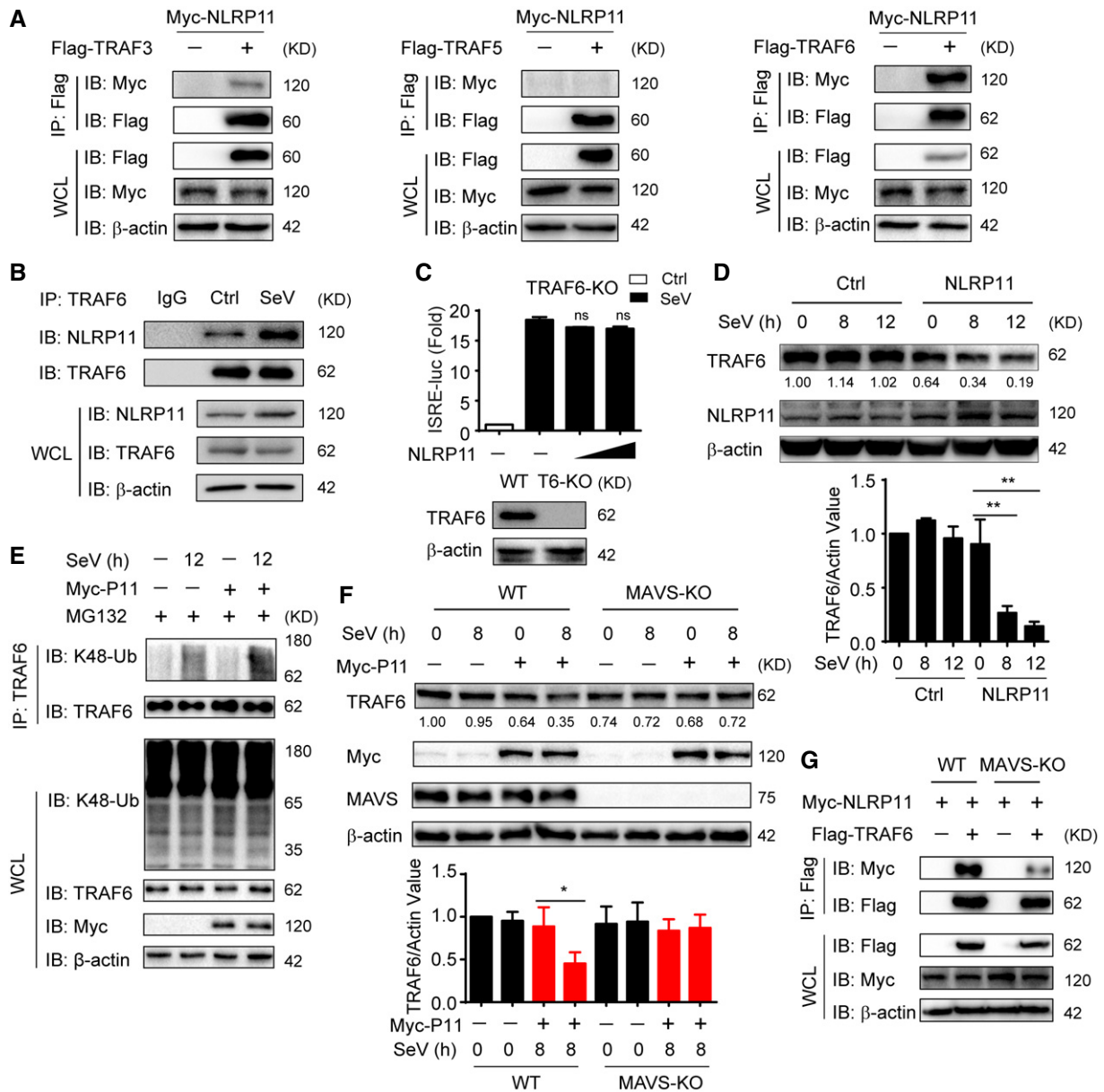


Figure 4. NLRP11 promotes TRAF6 degradation in a MAVS-dependent manner.

A 293T cells were transfected with Myc-NLRP11 and Flag-TRAF3, Flag-TRAF5, or Flag-TRAF6 for 24 h, and cell lysates were subjected to immunoprecipitation with anti-Flag beads, followed by immunoblot analysis with indicated antibodies.

B NLRP11 and TRAF6 interaction was analyzed by co-immunoprecipitation assay in THP-1 monocytes upon Sendai virus (SeV) (MOI = 1) infection for 20 h.

C Luciferase activity in *TRAF6* knockout (KO) 293T cells (bottom) transfected with ISRE promoter reporter and pRL-TK plasmid and increasing amount of NLRP11 followed by SeV (MOI = 0.1) infection for 20 h. Data are expressed as means \pm SEM of three independent experiments, versus cells transfected with EV with the same treatment, Student's *t*-test, ns: no significant.

D Immunoblot analysis of indicated proteins in *NLRP11* overexpressing THP-1 cells followed with SeV (MOI = 1) infection for indicated time points (top). Numbers between two blots indicate densitometry of TRAF6 relative to that of β -actin. Three independent experiments were quantified (bottom). Data are expressed as means \pm SD of three independent experiments (***P* < 0.01 versus uninfected cells, Student's *t*-test).

E 293T cells were transfected with empty vector or Myc-NLRP11 for 12 h, infected with SeV (MOI = 1) for 12 h, and then subjected to MG132 treatment for 6 h before harvesting. The cell lysates were subjected to immunoprecipitation with anti-TRAF6 antibody followed by immunoblot analysis with indicated antibodies.

F Wild-type (WT) and *MAVS* KO 293T cells were transfected with empty vector or Myc-NLRP11 for 24 h, and the cells were then infected with SeV (MOI = 0.1) for indicated time points. Cell lysates were subjected to immunoblot analysis with indicated antibodies (top). Numbers between two blots indicate densitometry of TRAF6 relative to that of β -actin. Three independent experiments were quantified (bottom). Data are expressed as means \pm SD of three independent experiments (**P* < 0.05 versus uninfected cells with the same treatment, Student's *t*-test).

G WT and *MAVS* KO 293T cells were transfected with Myc-NLRP11 and Flag-TRAF6 for 24 h, and the cell lysates were analyzed by immunoprecipitation assay.

Source data are available online for this figure.

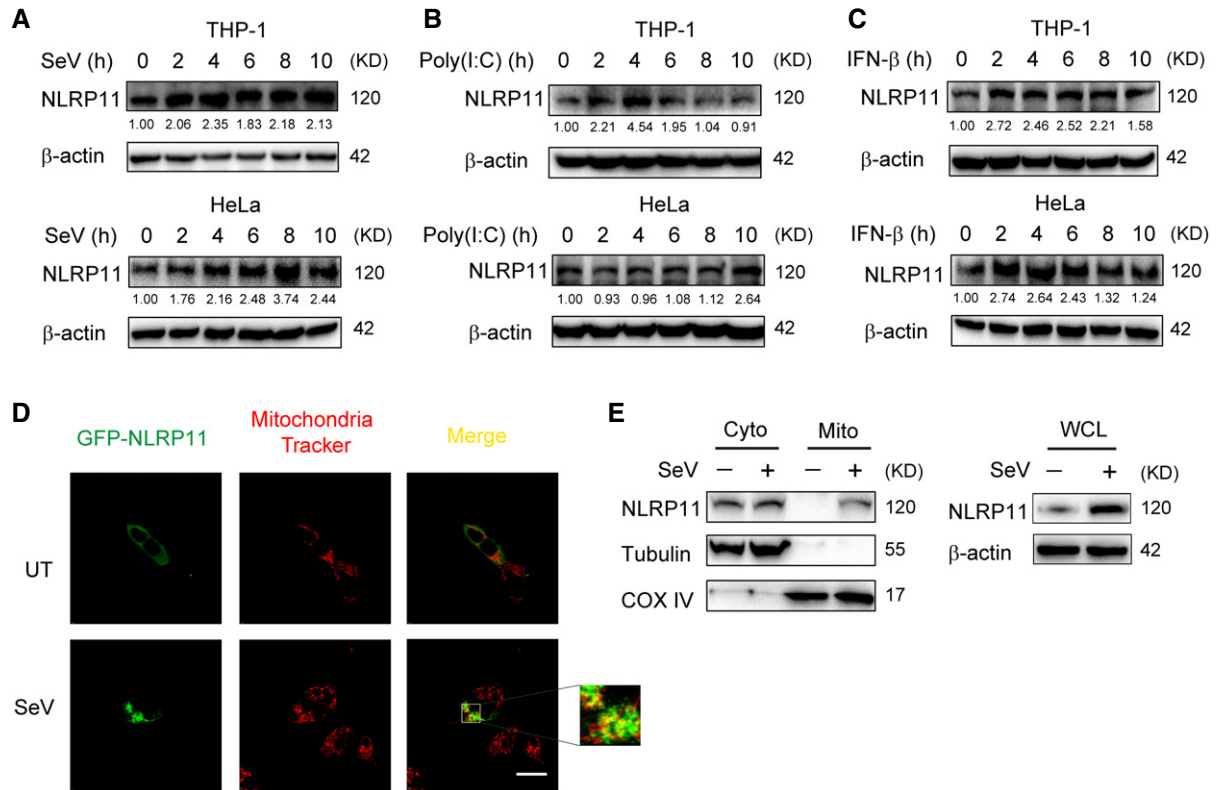


Figure 5. NLRP11 is induced and aggregated to mitochondria by type I IFNs.

A–C Immunoblot analysis of NLRP11 protein expression in THP-1 monocytes and HeLa cells infected with Sendai virus (SeV) (MOI = 1), transfected with poly(I:C) (10 μ g/ml), or treated with IFN- β (1,000 U/ml) for indicated time points. Numbers between two blots indicate densitometry of NLRP11 relative to that of β -actin.
 D 293T cells were transfected with GFP-NLRP11, and then were left untreated (UT) or infected with SeV (MOI = 1) for 12 h, followed by confocal fluorescence microscopy analysis. Mitochondria were detected with mitochondria tracker (red). Scale bar, 20 μ m.
 E HeLa cells were infected with SeV (MOI = 1) or not for 12 h, and then subjected to mitochondria isolation using cell mitochondria isolation kit (Beyotime Biotechnology) followed by immunoblot analysis. Tubulin and COX IV serve as cytosolic and mitochondrial markers, respectively.

Source data are available online for this figure.

Figure 6. NLRP11 suppresses virus-induced apoptosis.

A Wild-type (WT) and *NLRP11* knockout (KO) THP-1 cells were infected VSV-eGFP (MOI = 10) for 24 h or not, and then stained with trypan blue.
 B WT and *NLRP11* KO THP-1 cells were infected with VSV-eGFP (MOI = 10) for 12 h, and then stained with propidium iodide (PI), followed by fluorescence analysis. Scale bar, 100 μ m.
 C WT and *NLRP11* KO THP-1 cells were infected with VSV-eGFP (MOI = 10) for 24 h, and then subjected to PI staining analysis by flow cytometry. The eGFP-positive (infected) cells were gated to compare the cell death. Numbers indicated the percentage of PI-stained cells (left). Three independent experiments were quantified (right).
 D Cleaved PARP (C-PARP) was analyzed by immunoblot analysis in 293T cells transfected with empty vector or Myc-NLRP11 upon VSV-eGFP (MOI = 10) infection for 18 h.
 E Wild-type (WT) and *MAVS* KO 293T cells were transfected with empty vector or Myc-NLRP11, and then infected with VSV-eGFP (MOI = 10) for 18 h. C-PARP was analyzed by immunoblot analysis.
 F Cleaved PARP (C-PARP) was analyzed by immunoblot analysis in WT or *NLRP11* KO THP-1 cells upon VSV-eGFP (MOI = 10) infection for 24 h.
 G HT1080 cells were transfected with *NLRP11* siRNAs or negative control (NC) siRNA for 48 h, and then transfected with poly(I:C) (5 μ g/ml) for 24 h. Cells were harvested for immunoblot analysis (left). Three independent experiments were quantified (right). Numbers between two blots indicate densitometry of C-PARP relative to that of β -actin.
 H HT1080 cells were transfected with *NLRP11* siRNAs or negative control (NC) siRNA for 48 h, and then transfected with poly(I:C) (5 μ g/ml) for 24 h. Cells were harvested for Annexin V and PI staining analysis by flow cytometry.
 I HT1080 cells were transfected with Myc-NLRP11 and *TRAF6* siRNAs or negative control (NC) siRNA for 48 h, and then transfected with poly(I:C) (5 μ g/ml) for 24 h were harvested for immunoblot analysis.
 J A proposed model for the regulatory functions of NLRP11.

Data information: Data are expressed as means \pm SEM (A, C) or means \pm SD (G) of three independent experiments (* P < 0.05, ** P < 0.01, and *** P < 0.001, versus WT cells with the same treatment (A, C) or versus cells transfected with NC siRNA (G), Student's *t*-test).

Source data are available online for this figure.

that TRAF6 deficiency reduced IFN- β expression in both mouse and human cells, and Liu *et al* [23] found TRAF6 was an IRF3 activator, and knockdown of *TRAF6* reduced phosphorylation and dimerization of IRF3 in mouse cells. Based on these reports, we suggested that TRAF6 might function differently in different cell types or in response to different stimuli. Besides triggering apoptosis, virus could also activate pyroptosis in monocytes, macrophages, and dendritic cells [31]. In our study, NLRP11 inhibits virus-induced cell

death and apoptosis in THP-1 cells (Fig 6A–C and F), and whether NLRP11 affects pyroptosis needs further investigation.

In this study, we found NLRP11 played a dual regulatory role in virus-induced IFN production and apoptosis in a MAVS-dependent manner (Figs 4F and G, and 6E). Based on the experimental data, we proposed a working model to illustrate how NLRP11 could regulate virus-triggered type I IFN and apoptosis signaling pathways (Fig 6J). After viral infection, NLRP11 expression is induced and

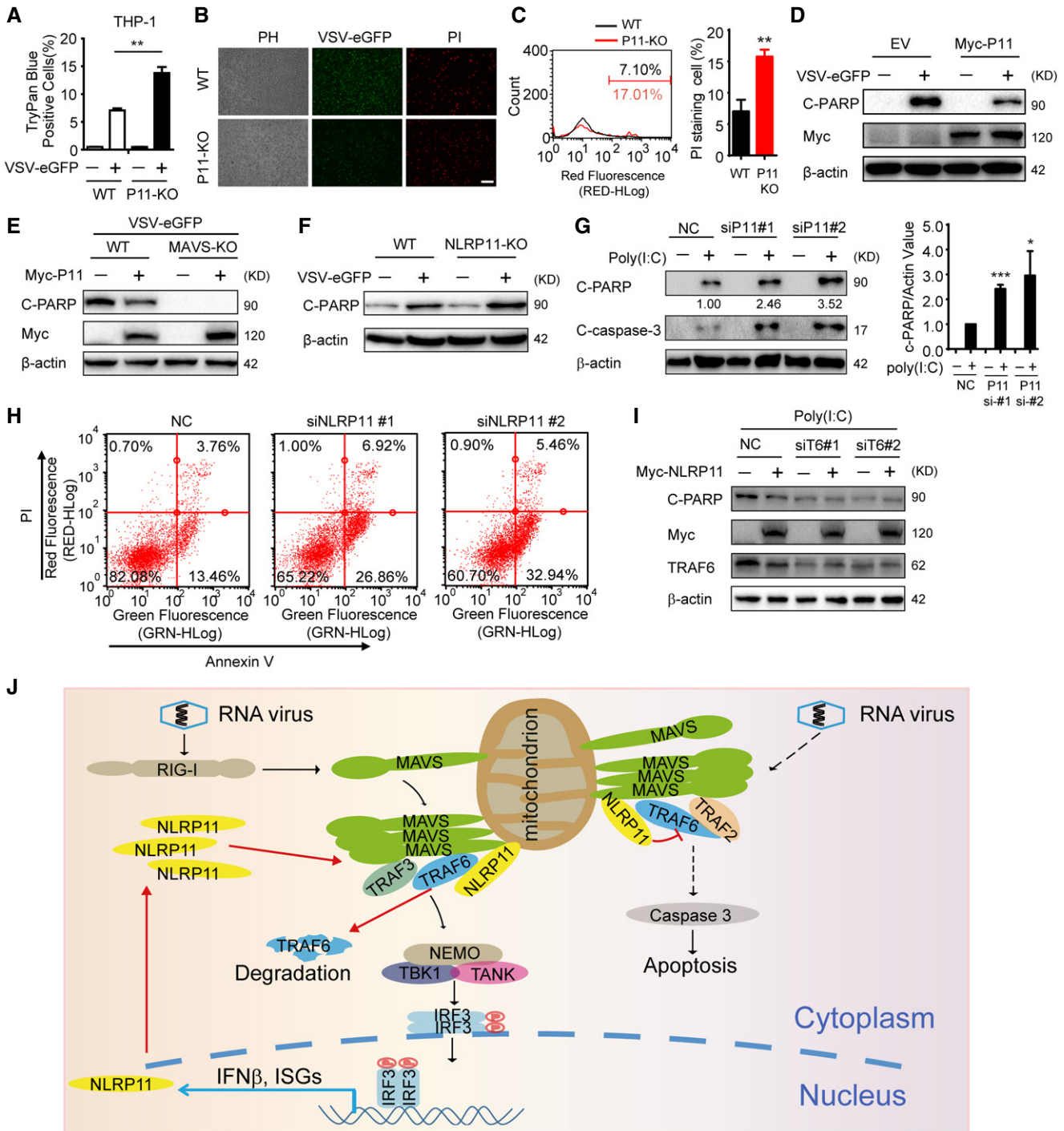


Figure 6.

translocates to mitochondria to target MAVS. Using MAVS as a platform, NLRP11 binds with TRAF6 to promote its degradation, and thus reduces type I IFN signaling. Along with the degradation of TRAF6, virus-induced apoptosis is also decreased.

Multiple proteins, such as several E3 ubiquitin ligases, including TRIM38, WWP1, and STUB1, are identified to mediate the degradation of TRAF6 by proteasome-dependent pathway [32–34]. Since NLRP11 is not an E3 ubiquitin ligase, whether NLRP11 recruits other E3 ligases to degrade TRAF6 needs further investigation. In summary, our study identifies NLRP11 as a negative regulator of type I IFN and virus-induced apoptosis via disrupting the activity of MAVS signalosome. NLRP11 might be used as a therapeutic target for inflammatory or autoimmune diseases, which were associated with aberrant RLR activation.

Materials and Methods

Antibodies

The following antibodies were used in this study: anti-IRF3 (sc-9082), donkey anti-goat IgG-HRP (sc-2020), goat anti-rabbit IgG-HRP (sc-2004), goat anti-mouse IgG-HRP (sc-2005), tubulin (sc-8035), MAVS (sc-166583), TRAF6 (sc-8409) (Santa Cruz Biotechnology); horseradish peroxidase (HRP)-anti-Flag (M2) (A8592), and anti- β -actin (A1978) (Sigma); HRP-anti-hemagglutinin (clone 3F10), anti-Myc-HRP (11814150001), unlabeled anti-Myc (11667203001) (Roche Applied Science); NLRP11 (NBP-1-92186) (Novus Biologicals); anti-p-IRF3 (#4947S), c-PARP (#5625), caspase-3 (#9661), TRAF6 (#8028), MAVS (#3993), mouse anti-rabbit IgG-HRP (#5127), K48-Ub-HRP (#12805), K63-Ub-HRP (#12930) (CST); NLRP11 (ab88732), COX IV (ab16056) (Abcam).

Virus infection

VSV-eGFP was kindly provided by Dr. Xiaofeng Qin (Suzhou Institute of Systems Medicine), and herpes simplex virus type 1 (HSV-1, KOS strain) was kindly provided by Dr. Guoying Zhou (Guangzhou Medical University). Cells were infected at various MOI, as previously described [35].

Real-time PCR

Total RNA was extracted using TRIzol reagent (Invitrogen) and reverse-transcribed using oligo-dT primers and reverse transcriptase (TAKARA). Real-time quantitative PCR was performed using SYBR green qPCR Mix kit (Genstar) and specific primers using the Primer 5.0 analyzer (Applied Biosystems). Data were normalized to the *Rpl13a* gene, and the relative abundance of transcripts was calculated by the $2^{-\Delta\Delta Ct}$ models. The sequences of primers are as follows:

IFNB1: Forward 5'-TGATACTCCTGGCACAAAT-3'
Reverse 5'-TTGAGCCTTCTGGAAGTGT-3'
ISG54: Forward 5'-GGAGGGAGAAAACCTCCTTGA-3'
Reverse 5'-GGCCAGTAGGTTGCACATTGT-3'
ISG56: Forward 5'-TCAGGTCAAGGATAGTCTGGAG-3'
Reverse 5'-AGGTTGTGATTCCACACTGTA-3'
SeV phosphoprotein: Forward 5'-GACGCGAGTTATGTGTTTGC-3'

Reverse 5'-TTCCACGCTCTCTTGGATCT-3'
TNFA: Forward 5'-CCAGACCAAGGTCAACCTCC-3'
Reverse 5'-CAGACTCGGCAAAGTCGAGA-3'
IL6: Forward 5'-AGAGGCACTGGCAGAAAACAAC-3'
Reverse 5'-AGGCAAGTCTCCTCATTGAATCC-3'
Rpl13a: Forward 5'-GCCATCGTGGCTAAACAGGTA-3'
Reverse 5'-GTTGGTGTTCATCCGCTTGC-3'

Immunoprecipitation and immunoblot analysis

Chemiluminescent HRP substrate (MILLIPORE) was used for protein detection, and ChemiDoc™ XRS+ imaging system (BIO-RAD) was used for immunoblot imaging. Procedures were done as previously described [36].

Luciferase reporter assays

293T (2×10^5) cells were seeded in 24-well plates and transfected with plasmids encoding an IFN- β or ISRE luciferase reporter (firefly luciferase; 100 ng) and pRL-TK (renilla luciferase plasmid; 10 ng), together with various amounts of the appropriate control or protein-expressing plasmid(s). An empty vector (pcDNA3.1) was used to maintain equal amounts of DNA among wells. Cells were collected at 24–36 h after transfection, and luciferase activity was measured with a dual-luciferase assay (Promega) with a Luminoskan Ascent luminometer (Thermo Scientific) according to the manufacturer's protocol. Reporter gene activity was determined by normalizing to renilla luciferase activity as previously described [16].

RNA interference

LipoRNAiMAX (Invitrogen) was used for transfection of siRNAs into cells, according to the manufacturer's instructions. The sequences of siRNAs are as follows:

NLRP11-siRNA-1#: Sense: GCGAUUCUCUCAUAUAUUTT
Antisense: AUUAUUGACAGUAUUGCCTT
NLRP11-siRNA-2#: Sense: GCCAUGAGAACGUCAAAUAATT
Antisense: UAUUUGACGUUCUCAUGGCTT
TRAF6-siRNA-1#: Sense: GCGCUGUGCAAACUAUAUATT
Antisense: UAUUAUAGUUUGCAGCGCTT
TRAF6-siRNA-2#: Sense: GCGCUUGCACCUUCAGUUATT
Antisense: UAACUGAAGGUGCAAGCGCTT
Negative control siRNA: Sense: UUCUCCGAACGUGUCACGUTT
Antisense: ACGUGACACGUUCGGAGAATT

Generation of knockout cells by CRISPR/Cas9 technology

293T or THP-1 knockout cells were generated by a CRISPR/Cas9 system, and the sequences of target sgRNAs are as follows:

NLRP11-sgRNA: Sense: GCTTGCTGAGCTAATCGCCA
Antisense: TGGCGATTAGCTCAGCCAAGC

TRAF6-sgRNA: Sense: CGTCTCGGCGCGCAGTGTCT
 Antisense: AGACACTGCGCGCCGAGACG
 MAVS-sgRNA: Sense: GATTGCGGCAGATATACTTAT
 Antisense: ATAAGTATATCTGCCGCAATC

Statistical analysis

Data are represented as mean \pm SEM or mean \pm SD when indicated, and Student's *t*-test was used for all statistical analyses. Differences between groups were considered significant when *P*-value was < 0.05 .

Expanded View for this article is available online.

Acknowledgements

This work was supported by National Natural Science Foundation of China (31370869, 31522018, and 31601135), National Key Basic Research Program of China (2014CB910800 and 2015CB859800). Yunfei Qin is partially supported by Outstanding Young Talent Research Fund of Zhengzhou University (F0000953), and the Startup Research Fund of Zhengzhou University (F0000922).

Author contributions

JC designed the research; YQ, ZS, YW, WX, and SJ performed the research; CW, WJ, and RZ provided technical help; and JC, YQ, YW, and ZS analyzed the data and wrote the manuscript.

Conflict of interest

The authors declare that they have no conflict of interest.

References

- Akira S, Uematsu S, Takeuchi O (2006) Pathogen recognition and innate immunity. *Cell* 124: 783–801
- Yoneyama M, Fujita T (2009) RNA recognition and signal transduction by RIG-I-like receptors. *Immunol Rev* 227: 54–65
- Wu B, Hur S (2015) How RIG-I like receptors activate MAVS. *Curr Opin Virol* 12: 91–98
- Hou F, Sun L, Zheng H, Skaug B, Jiang QX, Chen ZJ (2011) MAVS forms functional prion-like aggregates to activate and propagate antiviral innate immune response. *Cell* 146: 448–461
- Vazquez C, Horner SM (2015) MAVS coordination of antiviral innate immunity. *J Virol* 89: 6974–6977
- Seth RB, Sun LJ, Ea CK, Chen ZJ (2005) Identification and characterization of MAVS, a mitochondrial antiviral signaling protein that activates NF- κ B and IRF3. *Cell* 122: 669–682
- Chattopadhyay S, Sen GC (2017) RIG-I-like receptor-induced IRF3 mediated pathway of apoptosis (RIPA): a new antiviral pathway. *Protein Cell* 8: 165–168
- Chattopadhyay S, Kuzmanovic T, Zhang Y, Wetzel JL, Sen GC (2016) Ubiquitination of the transcription factor IRF-3 activates RIPA, the apoptotic pathway that protects mice from viral pathogenesis. *Immunity* 44: 1151–1161
- Chattopadhyay S, Yamashita M, Zhang Y, Sen GC (2011) The IRF-3/Bax-mediated apoptotic pathway, activated by viral cytoplasmic RNA and DNA, inhibits virus replication. *J Virol* 85: 3708–3716
- Lei Y, Moore CB, Liesman RM, O'Connor BP, Bergstralh DT, Chen ZJJ, Pickles RJ, Ting JPY (2009) MAVS-mediated apoptosis and its inhibition by viral proteins. *PLoS ONE* 4: e5466
- Chen G, Shaw MH, Kim YG, Nunez G (2009) NOD-like receptors: role in innate immunity and inflammatory disease. *Annu Rev Pathol-Mech* 4: 365–398
- Shaw MH, Reimer T, Kim YG, Nunez G (2008) NOD-like receptors (NLRs): bona fide intracellular microbial sensors. *Curr Opin Immunol* 20: 377–382
- Caruso R, Warner N, Inohara N, Nunez G (2014) NOD1 and NOD2: signaling, host defense, and inflammatory disease. *Immunity* 41: 898–908
- Lechtenberg BC, Mace PD, Riedl SJ (2014) Structural mechanisms in NLR inflammasome signaling. *Curr Opin Struct Biol* 29: 17–25
- Cui J, Zhu L, Xia XJ, Wang HY, Legras X, Hong J, Ji JB, Shen PP, Zheng S, Chen ZJJ et al (2010) NLRC5 negatively regulates the NF- κ B and type I interferon signaling pathways. *Cell* 141: 483–496
- Cui J, Li Y, Zhu L, Liu D, Songyang Z, Wang HY, Wang RF (2012) NLRP4 negatively regulates type I interferon signaling by targeting the kinase TBK1 for degradation via the ubiquitin ligase DTX4. *Nat Immunol* 13: 387–395
- Xia XJ, Cui J, Wang HLY, Zhu L, Matsueda S, Wang QF, Yang XA, Hong J, Songyang Z, Chen ZJJ et al (2011) NLRX1 negatively regulates TLR-induced NF- κ B signaling by targeting TRAF6 and IKK. *Immunity* 34: 843–853
- Lin M, Zhao ZY, Yang ZF, Meng QC, Tan P, Xie WH, Qin YF, Wang RF, Cui J (2016) USP38 inhibits type I interferon signaling by editing TBK1 ubiquitination through NLRP4 signalosome. *Mol Cell* 64: 267–281
- Zhang L, Mo J, Swanson KV, Wen H, Petrucelli A, Gregory SM, Zhang Z, Schneider M, Jiang Y, Fitzgerald KA et al (2014) NLRC3, a member of the NLR family of proteins, is a negative regulator of innate immune signaling induced by the DNA sensor STING. *Immunity* 40: 329–341
- Tian X, Pascal G, Monget P (2009) Evolution and functional divergence of NLRP genes in mammalian reproductive systems. *BMC Evol Biol* 9: 202
- Cai X, Chiu YH, Chen ZJ (2014) The cGAS-cGAMP-STING pathway of cytosolic DNA sensing and signaling. *Mol Cell* 54: 289–296
- Shalem O, Sanjana NE, Hartenian E, Shi X, Scott DA, Mikkelsen TS, Heckl D, Ebert BL, Root DE, Doench JG et al (2014) Genome-scale CRISPR-Cas9 knockout screening in human cells. *Science* 343: 84–87
- Liu S, Chen J, Cai X, Wu J, Chen X, Wu YT, Sun L, Chen ZJ (2013) MAVS recruits multiple ubiquitin E3 ligases to activate antiviral signaling cascades. *Elife* 2: e00785
- Barber GN (2001) Host defense, viruses and apoptosis. *Cell Death Differ* 8: 113–126
- Chattopadhyay S, Marques JT, Yamashita M, Peters KL, Smith K, Desai A, Williams BRG, Sen GC (2010) Viral apoptosis is induced by IRF-3-mediated activation of Bax. *EMBO J* 29: 1762–1773
- Kopecky SA, Willingham MC, Lyles DS (2001) Matrix protein and another viral component contribute to induction of apoptosis in cells infected with vesicular stomatitis virus. *J Virol* 75: 12169–12181
- Allen IC, Wilson JE, Schneider M, Lich JD, Roberts RA, Arthur JC, Woodford RMT, Davis BK, Uronis JM, Herfarth HH et al (2012) NLRP12 suppresses colon inflammation and tumorigenesis through the negative regulation of noncanonical NF- κ B signaling. *Immunity* 36: 742–754
- Lukens JR, Gurung P, Shaw PJ, Barr MJ, Zaki MH, Brown SA, Vogel P, Chi H, Kanneganti TD (2015) The NLRP12 sensor negatively regulates

- autoinflammatory disease by modulating interleukin-4 production in T cells. *Immunity* 42: 654–664
29. Moore CB, Bergstralh DT, Duncan JA, Lei Y, Morrison TE, Zimmermann AG, Accavitti-Loper MA, Madden VJ, Sun LJ, Ye ZM *et al* (2008) NLRX1 is a regulator of mitochondrial antiviral immunity. *Nature* 451: 573–577
 30. Chen H-W, Yang Y-K, Xu H, Yang WW, Zhai ZH, Chen DY (2015) Ring finger protein 166 potentiates RNA virus-induced interferon- β production via enhancing the ubiquitination of TRAF3 and TRAF6. *Sci Rep* 5: 14770
 31. Danthi P (2016) Viruses and the diversity of cell death. *Annu Rev Virol* 3: 533–553
 32. Zhao W, Wang L, Zhang M, Yuan C, Gao C (2012) E3 ubiquitin ligase tripartite motif 38 negatively regulates TLR-mediated immune responses by proteasomal degradation of TNF receptor-associated factor 6 in macrophages. *J Immunol* 188: 2567–2574
 33. Lin XW, Xu WC, Luo JG, Guo XJ, Sun T, Zhao XL, Fu ZJ (2013) WW domain containing E3 ubiquitin protein ligase 1 (WWP1) negatively regulates TLR4-mediated TNF- α and IL-6 production by proteasomal degradation of TNF receptor associated factor 6 (TRAF6). *PLoS ONE* 8: e67633
 34. Li S, Shu B, Zhang YQ, Li J, Guo JW, Wang YY, Ren FL, Xiao G, Chang ZJ, Chen D (2014) Carboxyl terminus of Hsp70-interacting protein regulation of osteoclast formation in mice through promotion of tumor necrosis factor receptor-associated factor 6 protein degradation. *Arthritis Rheumatol* 66: 1854–1863
 35. Chen M, Meng Q, Qin Y, Liang P, Tan P, He L, Zhou Y, Chen Y, Huang J, Wang RF *et al* (2016) TRIM14 inhibits cGAS degradation mediated by selective autophagy receptor p62 to promote innate immune responses. *Mol Cell* 64: 105–119
 36. Qin Y, Liu Q, Tian S, Xie W, Cui J, Wang RF (2016) TRIM9 short isoform preferentially promotes DNA and RNA virus-induced production of type I interferon by recruiting GSK3 β to TBK1. *Cell Res* 26: 613–628